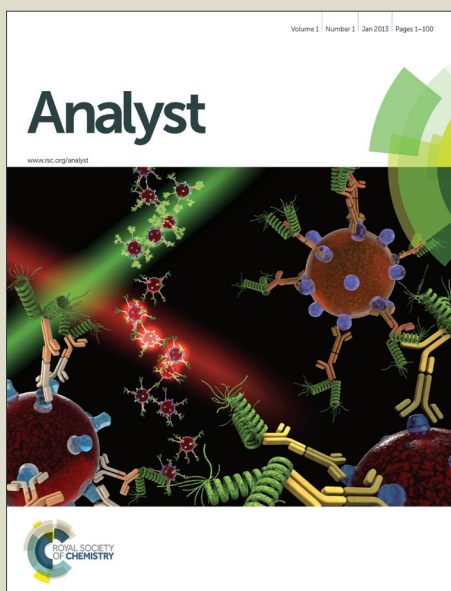


Analyst

Accepted Manuscript



This is an *Accepted Manuscript*, which has been through the Royal Society of Chemistry peer review process and has been accepted for publication.

Accepted Manuscripts are published online shortly after acceptance, before technical editing, formatting and proof reading. Using this free service, authors can make their results available to the community, in citable form, before we publish the edited article. We will replace this *Accepted Manuscript* with the edited and formatted *Advance Article* as soon as it is available.

You can find more information about *Accepted Manuscripts* in the [Information for Authors](#).

Please note that technical editing may introduce minor changes to the text and/or graphics, which may alter content. The journal's standard [Terms & Conditions](#) and the [Ethical guidelines](#) still apply. In no event shall the Royal Society of Chemistry be held responsible for any errors or omissions in this *Accepted Manuscript* or any consequences arising from the use of any information it contains.

Cite this: DOI: 10.1039/c0xx00000x

www.rsc.org/xxxxxx

COMMUNICATION

Contact Angle Changes Induced by Immunocomplex Formation†

Jong-Hoon Kim,^a Amy Q. Shen,^a Kyong-Hoon Lee,^b Gerard A. Cangelosi^c and Jae-Hyun Chung^{*a}

Received (in XXX, XXX) Xth XXXXXXXXX 20XX, Accepted Xth XXXXXXXXX 20XX

DOI: 10.1039/b000000x

5 **Immunoassays analyzing interactions between antigens and antibodies can be affected by capillary action together with binding affinity. This paper studies contact-angle changes of bacterial suspensions on antibody immobilized surfaces. The capillary action and the dried pattern of the cell suspensions are analyzed and correlated with specific- and nonspecific bindings between bacteria and antibodies.**

Introduction

One of the most significant challenges in global health is to diagnose infectious diseases accurately and economically in developing countries.¹ Early detection and treatment of highly contagious diseases such as *tuberculosis* are critical to patient care and control of disease transmissions. For the rapid identification of target biomarkers and microbial pathogen cells, immunoassays have frequently been used. Immunoassays rely on the abilities of antibodies to recognize and bind to specific target antigen molecules. For antibody characterization, an enzyme-linked immunosorbent assay (ELISA) is one of the reliable and relatively straightforward methods. However, ELISA requires large volumes of reagents and long incubation time. In addition, the assay results highly depends on manual practices, which can be a major error source.

When running an immunoassay, antibodies are immobilized on a substrate, often by incubation of a liquid drop. Target molecules are also bound in the similar format. In the process, the biological particles can form various patterns including ring-shaped structures, central bumps, uniform deposits, or complex patterns involving multiple rings and a network of polygons on the substrate.²⁻⁴ The deposit pattern is related to the surface energy interaction between the substrate and the liquid and the evaporation rate of the liquid.⁵ The drying patterns have been exploited for crystal formation of dispersed molecules.⁶⁻⁸ One of the most studied drying patterns is termed *coffee ring*.⁸ Over the past decade, various physical factors including pinning criteria,^{9, 10} particle size,¹¹ particle shape,¹² solvent type,¹³ and surfactant effects¹⁴ have been found to affect the coffee ring pattern. The coffee-ring effect can be manipulated for various applications including microarray deposition,⁷ ink jet printing,¹⁵ and particle separation.¹⁶ In the context of immunoassays or similar applications, the drying pattern can significantly affect assay performance due to the nonuniformly functionalized surfaces

with antibodies.¹⁷⁻²⁰ Recent studies also showed that the coffee ring patterns created from liquid drops containing bio-entities, such as protein molecules, micro-organisms, and cells could be utilized as biological indicators.^{11, 16} However, the impact of immunocomplex formation on the coffee ring patterns has yet to be studied.

In this paper, contact angles and deposit patterns of bacterial cell suspensions on antibody-coated surfaces are investigated in the context of antibody-antigen binding affinity. A rectangular gold substrate immobilized with specific antibodies is utilized as a model system. Two bacterial cell types, *Escherichia coli* (*E. coli*) and the *Bacillus Calmette-Guérin* (BCG) strain of *Mycobacterium bovis*, are used with their corresponding antibodies.

Materials and methods

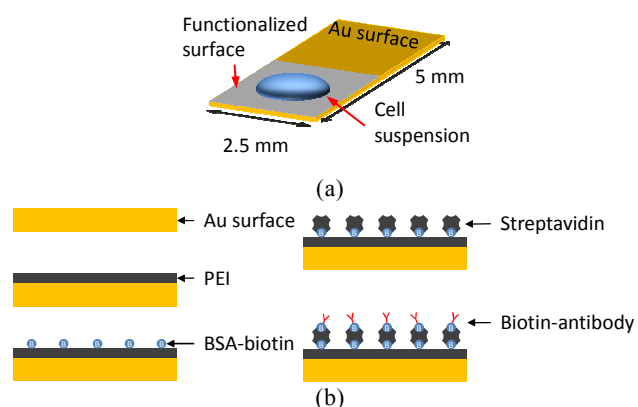


Fig. 1 (a) Schematics of experimental setup; (b) surface modification method depicting the sequential steps.

BCG and *E. coli* cells were chosen because of the similar sizes and shapes. Both cells were typically rod-shaped, and were about 2 μm in length and 0.5 μm in diameter. Anti-BCG polyclonal IgY antibodies were raised against *M. tuberculosis* complex (*M. bovis* BCG) cells,¹⁹ and the anti-*E. coli* polyclonal IgG antibodies were purchased from ProSci Inc

(Poway, CA). To investigate how the binding affinity affects the contact angle of a liquid drop containing bacterial cells, rectangular gold-coated Si substrates (2.5x5 mm²) were coated with antibodies (Fig. 1). On a Si wafer, a 500 nm-thick oxide layer was thermally grown. A 20 nm-thick gold layer was then

evaporated onto the oxide layer by electron-beam evaporation. The gold layer was then coated with polyethyleneimine (PEI, 1%, Sigma-Aldrich) by dipping the rectangular strip into a PEI solution for 1 minute. PEI was a water-soluble polymer that interacted strongly by hydrogen bond with proton donors. Since PEI was cationic, negatively charged proteins were attracted to the PEI-coated gold surface. The PEI-coated gold surface was dried at room temperature for 2 minutes. Subsequently, the PEI-coated gold surface was dipped into biotinylated bovine serum albumin (biotin-BSA, 10mg/mL, Sigma-Aldrich) for 5 minutes. Bovine serum albumin (BSA) was used as a blocker, to minimize non-specific interactions with the PEI-coated surface. Biotin was used as a linker to immobilize streptavidin. After drying the surface in air, streptavidin (1mg/mL, Sigma-Aldrich) was added to bind with the biotin-BSA-functionalized surface for 1 minute. Finally, the surface was functionalized with the biotinylated antibodies for 5 minutes, which bound tightly to streptavidin. Antibodies were either anti-BCG IgY or anti-*E. coli* IgG with the concentrations of 2 mg/mL. All the coating steps were conducted with dipping and withdrawal of the rectangular strip with speed of 100 $\mu\text{m}/\text{second}$. Note that lower concentration of antibodies can function in a similar way, but the lower concentration can cause the variation of the measurement potentially due to the non-uniform functionalization.

To visualize binding of bacterial cells on the functionalized surface, both BCG and *E. coli* cells at 10^7 cfu/mL in 1x phosphate buffered saline (PBS) buffer were stained with an intercalating dye (SYTO 9[®] green fluorescent nucleic acid stain; molecular probes L7007, Invitrogen, Carlsbad, CA). To eliminate unbound staining dyes, the solution was centrifuged to collect the pellet of stained cells. The supernatant was discarded. The collected pellets were resuspended in PBS. Stained BCG and *E. coli* cells were used for the contact angle measurement.

With two different types of antibody-coated substrate, the initial contact angles using 0.5 μL PBS buffer without bacteria were measured. To analyze the specific- and nonspecific binding cases, four combinations were tested as summarized in Table 1. A 0.5 μL -droplet of stained BCG or *E. coli* cells was deposited on the antibody functionalized substrate. After the placement of a droplet, the contact angle at the initial state and during evaporation were measured by using a goniometer (Rame-Hart, model 500 Adv G/T) in a given temperature and humidity because the evaporation speed can be changed due to the ambient condition. Each case was repeated three times ($n=3$). The ambient temperature and humidity during the measurement were 24.2 ± 0.49 $^{\circ}\text{C}$ and 23.2 ± 1.1 %, respectively. The dried pattern was then observed under a reflective light epi-fluorescence microscope at 10x magnification (Olympus BX-41, Olympus America Inc., Melville, NY, excitation and emission wavelength: 480 nm and 520nm, respectively). To evaluate the distribution of the bacteria, the fluorescence images were digitized on the basis of a threshold value by using Matlab[®]. The threshold value was used to eliminate the background signals. Note that the contact angle measurement was also conducted for drops of

BCG and *E. coli* suspension on gold surfaces. The contact angles between the bacterial cells were similar without antibodies (ESI[†], Fig. S1). According to this result, intracellular materials of both BCG and *E. coli* do not affect the outcome of contact angles.

Table 1. Summary for experimental combinations.

	Antibodies on substrate	
	BCG IgY antibodies	<i>E. coli</i> IgG antibodies
PBS	Buffer-BCG IgY: (θ_0) _{BCG-IgY}	Buffer- <i>E. coli</i> IgG: (θ_0) _{<i>E. coli</i>-IgG}
BCG	Specific-BCG IgY: (θ_{bs}) _{BCG-IgY}	Nonspecific- <i>E. coli</i> IgG: (θ_{bn}) _{<i>E. coli</i>-IgG}
<i>E. coli</i>	Nonspecific-BCG IgY: (θ_{bn}) _{BCG-IgY}	Specific- <i>E. coli</i> IgG: (θ_{bs}) _{<i>E. coli</i>-IgG}

Results and discussion

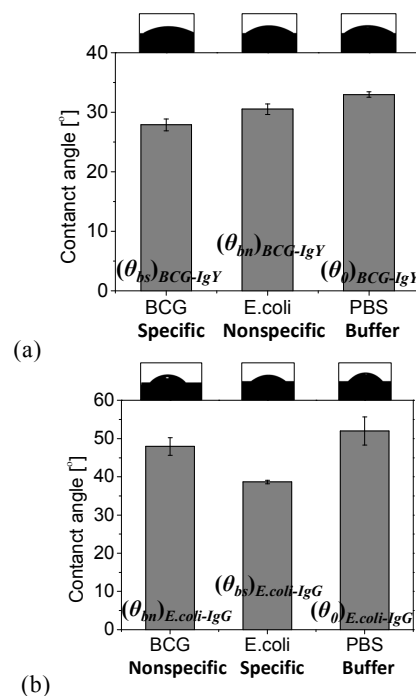


Fig. 2 Measurement of initial contact angles for both BCG and *E. coli* on surfaces functionalized with (a) anti-BCG IgY and (b) anti-*E. coli* IgG ($n=3$).

When the initial contact angle was measured for specific- and nonspecific bindings, the contact angle at specific bindings was reduced relative to that of nonspecific binding. When a liquid drop of PBS buffer was placed on a substrate with immobilized anti-BCG IgY antibodies, the contact angle without cells was 33° . Subsequently, when drops containing *E. coli* or BCG cells were placed on the anti-BCG IgY substrate, the contact angles were reduced to 31° and 27° , respectively (Fig. 2a). When the substrate was functionalized with anti-*E. coli* IgG, the contact angle with PBS alone was 52° . The

difference relative to anti-BCG IgY might reflect differences in the electric charge of antibodies. When droplets containing *E. coli* or BCG cells were placed on the anti-*E. coli* IgG substrate, the contact angles were reduced to 39° and 48°, respectively (Fig. 2b). With both antibodies, the contact angle was sequentially reduced from the pure PBS case, to the nonspecific case, and then to the specific case. The concentrations of bacterial cells can change the contact angle. However, the variations of one order of magnitude in the concentration do not make a significant change in the contact angle because the contact angle change between 0 (pure PBS) and 10⁷ cfu/mL (BCG or *E. coli*) is only 4~13 degrees. Thus, a sensitivity test using various concentrations of bacteria has not been conducted in this paper. The initial contact angle for each case was summarized in Table 2.

Regarding the specificity of both antibodies, an ELISA kit was used. Both antibodies bound more avidly to the corresponding target bacterial cells (ESI†, Fig. S2). The result was consistent with the contact angle measurement.

Table 2. Summary of the initial contact angles.

	Anti-BCG IgY functionalized surface	Anti- <i>E. coli</i> IgG functionalized surface
PBS	$(\theta_0)_{\text{BCG-IgY}}: 33^\circ$	$(\theta_0)_{\text{E. coli-IgG}}: 52^\circ$
BCG	$(\theta_{bs})_{\text{BCG-IgY}}: 27^\circ$	$(\theta_{bn})_{\text{E. coli-IgG}}: 48^\circ$
<i>E. coli</i>	$(\theta_{bn})_{\text{BCG-IgY}}: 31^\circ$	$(\theta_{bs})_{\text{E. coli-IgG}}: 39^\circ$

Contact angles gradually declined as evaporating liquid drops progressed. However, the general trend among all cases was maintained. Droplets with smaller initial contact angles showed faster evaporation. Due to the pinning effect, liquid drops of the specific binding cases always evaporated more quickly (ESI†, Fig. S3).

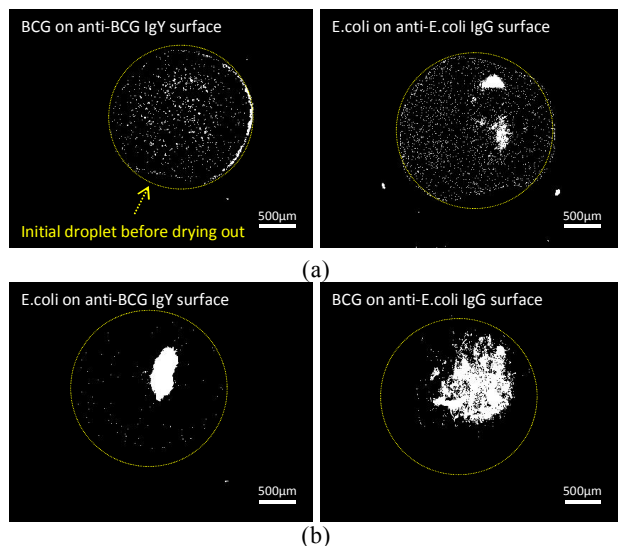


Fig. 3 Drying patterns for four different cases (a) specific binding case: target bacterial cells on the corresponding

antibody-coated surface; (b) nonspecific binding case: bacterial cells on the nonspecific antibody-coated surface. Yellow circles indicate the initial shape of droplets before the evaporation, and white dots are bacterial cells after dry.

During the evaporation of liquid drops containing target bacteria on the substrate, the bacterial cells were transported to the edge of the drops due to the pinning and the evaporation of the liquid (ESI†, Fig. S4; pinned mode). The larger binding forces for specific bindings held the contact line of the liquid drop, resulting in a coffee ring pattern of bacteria. The dried patterns of the cells were also compared for both specific and nonspecific cases. The specific binding cases showed more distinct coffee ring patterns. We speculate that the coffee ring effect is enhanced due to specific binding, which could align more target cells to the contact line as seen in Fig. 3a. For the nonspecific binding cases, the majority of the cells were accumulated in the middle of the droplet zone after evaporation (Fig. 3b).

To understand the relationship between the contact angle of the target cells on functionalized surfaces and specific binding, we analyzed the evaporation mechanism of liquid droplets containing the target bacteria and the functionalized surfaces. Liquid droplets on a given substrate can evaporate with two different modes. One is the receding mode where the contact area between the droplet and the substrate continuously decreases during evaporation (ESI†, Fig. S4a). In this mode, the contact angle can either decrease or stay as a constant. The alternative mode is the pinned mode, in which the contact area remains as a constant while the contact angle gradually decreases (ESI†, Fig. S4b). Evaporation, a complex and nonequilibrium phenomenon, occurs over the entire drop surface. In the receding mode, Marangoni flow is dominant, which results in a recirculatory flow. In the pinned mode, the contact angle decreases as the liquid drop evaporates. Thus, a capillary flow outward from the drop's center to its edges is induced to replenish evaporating liquid at the contact line. This action brings suspended particles to the edge as evaporation proceeds.

Upon specific binding, the binding forces are derived from Young-Laplace equation as below [ESI†, equation (s5)].

$$f_b = \gamma_{LG}[\cos\theta_b(t) - \cos\theta_0] - f'(t) \quad (1)$$

where f_b and $f'(t)$ are the binding forces at the steady state and during the evaporation, respectively. γ_{LG} is the liquid-vapor interfacial energy, $\cos\theta_b(t)$ is the contact angle in the presence of the binding, and $\cos\theta_0$ is the contact angle without bindings. Therefore, as the binding constant increases, the change of the contact angle will be increased by the stronger binding forces derived from a larger number of the immunocomplex. f_b can be estimated by equation (1) with the measurement of $\theta_b(0)$ and θ_0 at $t=0$ ($f'(t)=0$ at the steady state). The unit of f_b is force per unit length.

Specific binding between cells and antibodies shows higher binding forces than those of nonspecific binding.²¹ In the case of specific binding, the cells are more strongly pinned at the contact line of the droplet, which reduces the contact angle (θ_{bs}) and increases the evaporation flux due to the larger surface area. With nonspecific binding, the weakly pinned

contact line causes higher contact angle (θ_{bn}) and smaller evaporation flux. In the case of a strongly pinned contact line, the projected area of the droplet should be maintained with evaporation. Through outward flow as the volume of the droplet decreases, cells are transported to the contact line and thus form the relatively thick perimeter of cells¹³ (ESI†, Fig. S4c and Fig. S5). According to equation (1), the contact angles at $t=0$ should be reduced from the case of pure liquid (θ_0) to the case of nonspecific binding (θ_{bn}), finally to the case of specific binding (θ_{bs}), which shows qualitative agreement with our experiment results (Fig. 2 and ESI†, Fig. S3).

The binding force between antigen and antibody is determined by the measured contact angles at $t=0$. The surface tension of PBS buffer is measured to be 0.063 N/m (Tensiometer Sigma 700). It is assumed that the contact line is connected with bacterial cells without vacancy, and the size (d) of single binding site on the surface of bacterial cell is 33 nm.²² The size of d includes the size of a single antigen-antibody unit (20nm) and the gap between two binding sites (13 nm). The force per single antigen-antibody unit is $f_b \times d$. Based on the contact angles in Table 2 and equation (1), with $d=33$ nm, the computed binding forces are estimated to be 109 pN for BCG – BCG IgY and 336 pN for *E.coli* – *E.coli* IgG. These estimated values agree with the binding forces measured by an atomic force microscope (AFM) varying from 50 pN to 250 pN.²³⁻²⁵ The difference of the binding forces between BCG and *E.coli* may be caused by the different binding affinity of the antibodies. In summary, the specific binding between cells and antibodies induces the pinning of cells at the meniscus of the bacterial droplet, which reduces the contact angle and increases the evaporation flux. In the case of nonspecific bindings, the contact angle is reduced to a lesser degree. Based on the contact angle measurements of bacterial suspension on antibody immobilized surfaces, we can easily characterize the antibody without cumbersome ELISA tests and AFM measurements. The affinity of antibody can be evaluated by the difference of contact angles between specific- and nonspecific cases, and the avidity of antibody can be quantified by using the Young-Laplace equation with the measured contact angles.

Conclusions

The impact of immunocomplex formation on contact angles was investigated. At equilibrium, the contact angle for specific binding was smaller than that of nonspecific binding due to the binding forces associated with the immunocomplex formation. With evaporation, the higher binding force from specific binding more rapidly reduced the contact angle in comparison to the nonspecific binding case. The lower contact angle for the specific binding cases induced a strong outward flow to the edge of the liquid. Thus, the coffee-ring effect was enhanced in the presence of target cells, which aligned the target bacteria cells in a circular-ring pattern.

Acknowledgement

We gratefully acknowledge funding for this work provided by NSF Career (ECCS-0846454) and NIH NIAID (R01AI093418). We appreciate Scott Soelberg in Furlong's group at University of Washington for the ELISA tests.

Notes

^a Department of Mechanical Engineering, University of Washington, Seattle, WA, USA; E-mail: jae71@uw.edu

^b NanoFactory, Inc., P.O. Box 52651, Bellevue, WA, USA

^c Department of Environmental and Occupational Health Sciences, University of Washington, Seattle, WA

⁶⁵

*Corresponding Author

Jae-Hyun Chung: Tel/ Fax 1-206-543-4355/ 1-206-685-8047, E-mail: jae71@uw.edu

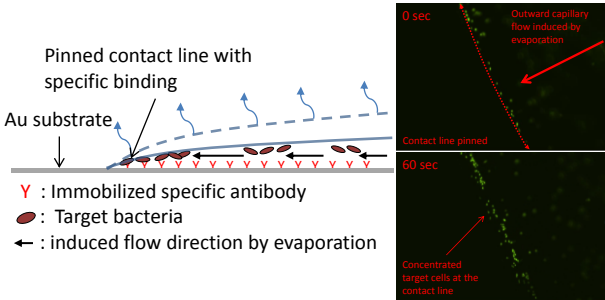
† Electronic supplementary information (ESI) available: (1) Transport of bacteria cells to the edge of a liquid drop on the antibody-coated surface., (2), (3), (4) and (5) are provided. See DOI: 10.1039/b000000x/

References

- H. Varmus, R. Klausner, E. Zerhouni, T. Acharya, A. S. Daar and P. A. Singer, *Science*, 2003, **302**, 398-399.
- T. T. Nellimoottil, P. N. Rao, S. S. Ghosh and A. Chattopadhyay, *Langmuir*, 2007, **23**, 8655-8658.
- W. Sempels, R. De Dier, H. Mizuno, J. Hofkens and J. Vermant, *Nat Commun*, 2013, **4**, 1757.
- J. T. Wen, C.-M. Ho and P. B. Lillehoj, *Langmuir*, 2013.
- R. Bhardwaj, X. H. Fang, P. Somasundaran and D. Attinger, *Langmuir*, 2010, **26**, 7833-7842.
- E. Rabani, D. R. Reichman, P. L. Geissler and L. E. Brus, *Nature*, 2003, **426**, 271-274.
- S. Choi, S. Stassi, A. P. Pisano and T. I. Zohdi, *Langmuir*, 2010, **26**, 11690-11698.
- R. D. Deegan, O. Bakajin, T. F. Dupont, G. Huber, S. R. Nagel and T. A. Witten, *Nature*, 1997, **389**, 827-829.
- A. S. Sangani, C. H. Lu, K. H. Su and J. A. Schwarz, *Phys Rev E*, 2009, **80**, 011603.
- Y.-F. Li, Y.-J. Sheng and H.-K. Tsao, *Langmuir*, 2013, **29**, 7802-7811.
- J. R. Trantum, D. W. Wright and F. R. Haselton, *Langmuir*, 2012, **28**, 2187-2193.
- P. J. Yunker, T. Still, M. A. Lohr and A. G. Yodh, *Nature*, 2011, **476**, 308-311.
- R. D. Deegan, O. Bakajin, T. F. Dupont, G. Huber, S. R. Nagel and T. A. Witten, *Phys Rev E*, 2000, **62**, 756-765.
- H. Hu and R. G. Larson, *Langmuir*, 2005, **21**, 3972-3980.
- D. Soltman and V. Subramanian, *Langmuir*, 2008, **24**, 2224-2231.
- T. S. Wong, T. H. Chen, X. Y. Shen and C. M. Ho, *Anal Chem*, 2011, **83**, 1871-1873.
- S. Gupta, S. Huda, P. K. Kilpatrick and O. D. Velev, *Anal Chem*, 2007, **79**, 3810-3820.
- J. W. Hong, K. H. Chung and H. C. Yoon, *Analyst*, 2008, **133**, 499-504.
- J. H. Kim, W. H. Yeo, Z. Q. Shu, S. D. Soelberg, S. Inoue, D. Kalyanasundaram, J. Ludwig, C. E. Furlong, J. J. Riley, K. M. Weigel, G. A. Cangelosi, K. Oh, K. H. Lee, D. Y. Gao and J. H. Chung, *Lab Chip*, 2012, **12**, 1437-1440.

-
20. Y. S. Gong, L. Chang, K. L. Viola, P. N. Lacor, M. P. Lambert, C. E. Finch, G. A. Krafft and W. L. Klein, *P Natl Acad Sci USA*, 2003, **100**, 10417-10422.
21. M.-P. Larvor, L. Djavadi-Ohanian, B. Nall and M. E. Goldberg, *J Immunol Methods*, 1994, **170**, 167-175.
22. R. M. Murphy, H. Slayter, P. Schurtenberger, R. A. Chamberlin, C. K. Colton and M. L. Yarmush, *Biophys J*, 1988, **54**, 45-56.
23. R. Ros, F. Schwesinger, D. Anselmetti, M. Kubon, R. Schafer, A. Pluckthun and L. Tiefenauer, *P Natl Acad Sci USA*, 1998, **95**, 7402-7405.
24. S. Allen, X. Y. Chen, J. Davies, M. C. Davies, A. C. Dawkes, J. C. Edwards, C. J. Roberts, J. Sefton, S. J. B. Tandler and P. M. Williams, *Biochemistry-Us*, 1997, **36**, 7457-7463.
25. U. Dammer, M. Hegner, D. Anselmetti, P. Wagner, M. Dreier, W. Huber and H. J. Guntherodt, *Biophys J*, 1996, **70**, 2437-2441.

TOC



Transport of bacteria cells to the edge of a liquid drop on the antibody-coated surface